An AKT1- and TRIM21-mediated Phosphodegron Controls Proteasomal Degradation of HuR Enabling Cell Survival under Heat Shock

Sharanya Nag
Indian Institute of Science Education and Research, Kolkata
Sayanur Rahaman
Indian Institute of Science Education and Research, Kolkata https://orcid.org/0000-0002-7526-7901
Abhishek Guha
Indian Institute of Science Education and Research, Kolkata
Partho Ray (psray@iiserkol.ac.in)
Indian Institute of Science Education and Research, Kolkata https://orcid.org/0000-0002-8795-3060

Article

Keywords:

Posted Date: June 23rd, 2022

DOI: https://doi.org/10.21203/rs.3.rs-1774410/v1

Abstract

Post-transcriptional regulation by RNA-binding proteins (RBPs) is a major mode of controlling gene expression under stress conditions. The RBP HuR regulates the translation and/or stability of mRNAs of multiple genes involved in stress responses. HuR is degraded in response to heat stress consequent to ubiquitination of the K182 amino acid residue. We have identified TRIM21 as the E3-ubiquitin ligase causing HuR polyubiquitination at K182 and proteasomal degradation under heat shock. TRIM21-mediated degradation of HuR protected cells from heat-shock induced cell death. By a combination of molecular dynamics simulation and experimentation we found the S100 and E101 residues to be required for binding of TRIM21 to HuR. Heat shock-induced phosphorylation of S100 was necessary for TRIM21 interaction with HuR and subsequent degradation. We identified AKT1 as the kinase which phosphorylates S100, allowing the recognition of HuR by TRIM21. Sequential phosphorylation by AKT1 and ubiquitination by TRIM21 therefore determine a “phosphodegron” in HuR that regulates the cellular level of HuR under heat shock, thereby enabling a crucial adaptive mechanism allowing cell survival in response to heat stress.

Introduction

Cellular stress activates multiple decision-making responses in gene expression pathways allowing cells to survive and adapt to stress conditions or undergo cell death[1]. Cellular stress responses therefore involve stress-specific transcriptional and post-transcriptional changes in gene expression[2,3]. Post-transcriptional regulation of gene expression is mediated by RNA-binding proteins (RBPs) and non-coding RNAs (ncRNAs) which regulate the translation and turnover of mRNAs[4–6]. Stress-induced regulation of RBP abundance and activity is therefore a widespread phenomenon of central importance in stress responses[7].

Heat shock response (HSR) is an evolutionarily conserved, fundamental stress response in organisms to cope with sudden changes in ambient temperature. Heat shock leads to deleterious effects on the cellular cytoskeleton together with unfolding of proteins, changes in cellular metabolism and gene expression, leading to cell cycle arrest[8]. Depending on duration and severity, heat stress can result in cell death[9]. Transcriptional and post-transcriptional changes in gene expression in heat-stressed cells lead to the altered expression of molecular chaperones and other regulators which enable the cells to cope with the stress[10–13]. As heat stress induces a global inhibition of translation, specific RBPs are regulated to ensure the continued stability and translation of a cohort of mRNAs required for the HSR[14–16]. Regulation of RBP levels and function is therefore crucial for HSR.

HuR or ELAVL1 is a ubiquitously expressed RBP involved in the cellular response to a variety of stress conditions[17–22]. HuR determines the cellular stress responses by regulating the stability and/or translation of mRNAs of multiple stress-responsive genes[23]. HuR is predominantly nuclear but translocates to the cytoplasm in response to most stress stimuli, where it exerts its post-transcriptional

effects on target mRNAs[24]. HuR undergoes partial nuclear-cytoplasmic translocation in response to heat shock at 45°C and localize in cytoplasmic foci[25]. Conversely, the majority of HuR was found to crosslink with nuclear poly(A) RNA in response to heat shock, suggesting that HuR gets trapped with nuclear mRNAs in heat-stressed cells [22]. Interestingly, mild heat shock at 43°C strongly reduced cellular HuR level by promoting the degradation of HuR through ubiquitination of the Lys182 (K182) residue[26]. Recently, K182 was also found to be the target of ubiquitination in HuR in response to UV irradiation[27]. However, neither the E3 ubiquitin ligase responsible for this heat shock-induced proteolysis of HuR, nor the specific post-translational modifications leading to the recognition by the E3 ligase have been identified.

In this study we have identified TRIM21 as the E3-ubiquitin ligase causing HuR poly-ubiquitination at K182 and proteasomal degradation under heat shock. The residues S100 and E101 were found to be crucial for the recognition of HuR by TRIM21. Remarkably, phosphorylation of S100 by the kinase AKT1 was required for the interaction with TRIM21. The AKT1 and TRIM21-mediated phosphorylation and degradation of HuR protected cells from heat-shock induced death. AKT1 and TRIM21 therefore determine a “phosphodegron” in HuR that is crucial for the degradation of HuR and the cellular response to thermal stress.

Results

The E3 ubiquitin ligase TRIM21 causes degradation of HuR in response to heat shock

Moderate heat shock, at 43°C for 2 h, to MCF7 cells in 10% serum-containing medium caused a strong time-dependent reduction of HuR protein to ~25% of initial level, with no change in mRNA level (**Fig. 1A**). Heat shock at 43°C to MCF7 cells in serum-free medium also caused a similar reduction in HuR protein level, as reported earlier in HeLa cells[26], suggesting that the HuR response to heat shock is independent of serum or cell type (**Suppl. Fig. 1**). Exogenously expressed EGFP-tagged HuR showed a similar reduction in response to heat shock (**Fig. 1B**). Both nuclear and cytoplasmic HuR showed similar degradation in heat-stressed cells, indicating cytoplasmic translocation as not a prerequisite for HuR degradation (**Suppl. Fig. 2**). Protein synthesis inhibition by cycloheximide (CHX) rapidly reduced HuR in heat-stressed cells compared to cells at 37 °C, demonstrating a significantly higher degradation rate of HuR under heat shock. However, treatment with the proteasomal inhibitor MG132, in presence of CHX, maintained the cellular level of HuR at 43°C (**Fig. 1C**). The half-life of HuR in heat-stressed cells treated with CHX goes down to ~30 min, whereas it is restored to more than 2 h on MG132 treatment (**Fig 1D**). This demonstrates that HuR is proteasomally degraded under heat shock.

As the K182 residue of HuR is reported to be polyubiquitinated under heat shock, we expressed 6X-His-tagged wild type (WT) and K182R mutant HuR proteins in cells and subjected them to heat shock. WT HuR was efficiently degraded, whereas K182R mutant HuR was protected from degradation under heat shock (**Fig 1E**). WT HuR underwent polyubiquitination in cells exposed to heat shock which was significantly reduced in case of the K182R mutant (**Fig. 1F**).

The K182 residue is polyubiquitinated by the ubiquitin ligase TRIM21 in response to UVC irradiation[27]. We therefore investigated whether TRIM21 was the E3-ligase responsible for degrading HuR under heat shock. HuR and TRIM21 showed interaction in cells at normal temperature and enhanced interaction in cells exposed to heat shock at 43°C for 1 h and treated with MG132 (**Fig. 1G**). siRNA-mediated depletion of TRIM21 prevented the degradation whereas overexpression of TRIM21 enhanced the degradation of HuR under heat shock (**Fig. 1H and 1I**).

To determine the involvement of K182 in the degradation of HuR by TRIM21 under heat shock, TRIM21 was co-expressed in cells expressing either myc-tagged WT or K182R mutant HuR. Upon heat shock, WT-HuR was degraded but the HuR K182R mutant was protected from degradation (**Fig. 1J**). K182R mutant HuR also showed significantly reduced interaction with TRIM21 upon heat shock (**Fig. 1K**). Together, these observations demonstrated TRIM21 as the E3 ubiquitin ligase causing the degradation of HuR under heat shock *via* the ubiquitination of K182.

TRIM21-mediated degradation of HuR protects cells from heat shock-induced cell death

TRIM21 enhances cell proliferation and reverses the DNA damage-induced cell death in UV-irradiated cells[28]. We therefore investigated the effect of TRIM21 on cell viability and death in response to heat shock. TRIM21 overexpression enhanced cell viability at 37°C and also significantly rescued the viability of heat-stressed cells (**Fig. 2A, left panel**). Conversely, TRIM21 depletion reduced cell viability and further accentuated the reduction of viability of heat-stressed cells (**Fig. 2A, right panel**). TRIM21 overexpression reduced caspase 3/7 activity in cells at 37°C and also significantly reduced the enhanced caspase activity in heat-stressed cells (**Fig. 2B, left panel**). The opposite effect was seen on TRIM21 knockdown (**Fig. 2B, right panel**). Annexin V/PI staining of cells overexpressing TRIM21 showed significant reduction in the enhanced apoptosis of cells exposed to heat shock (**Fig. 2C**). The converse was observed in cells in which TRIM21 was knocked down (**Fig. 2D**). This demonstrated that TRIM21 enhanced the viability and reduced apoptosis of heat- stressed cells.

We then investigated the effect of TRIM21 on the morphological changes of heat-stressed cells. Heat shock caused a visible change in cellular morphology in comparison to cells at 37°C (**Suppl. Fig. 3 and 4**). The reduction in cell area and perimeter upon heat shock were significantly restored on TRIM21 overexpression (**Fig. 2E**). Conversely, TRIM21 knockdown further reduced cell area and perimeter of heat stressed cells (**Fig. 2F**). TRIM21 also enhanced the long-term viability and proliferation of heat-stressed cells. TRIM21 overexpression significantly enhanced the proliferation of cells at 37°C over a 72 h period. While cells exposed to heat shock showed significantly reduced proliferation during this period, TRIM21 overexpression significantly enhanced the proliferation of heat-stressed cells and restored it nearly to the level of cells unexposed to heat shock (**Fig. 2G**). Depletion of TRIM21 showed the opposite effect (**Fig. 2H**). Heat-stressed cells formed significantly less number of colonies compared to cells not exposed to heat shock, whereas colony formation by heat-stressed cells overexpressing TRIM21 was nearly similar (**Fig. 2I**). Together, these observations demonstrated a profound role of TRIM21 in ensuring short term survival and long term viability of cells exposed to heat shock.

We thereafter investigated whether the survival advantage provided by TRIM21 under heat shock was mediated by its degradation of HuR. Overexpression of both WT HuR and HuR K182R, which is refractory to TRIM21-mediated degradation, significantly reduced the enhanced viability of cells observed on TRIM21 overexpression. WT HuR reduced the enhanced viability of heat-stressed cells overexpressing TRIM21 which was further reduced on overexpression of HuR K182R mutant (**Fig. 2J, left panel**). The opposite effect was observed in case of cellular caspase activity (**Fig. 2J, right panel**). This demonstrated that WT HuR, and more so the non-degradable K182R mutant HuR, could reverse the increase in cell viability and decrease in apoptosis induced by TRIM21 overexpression in heat-stressed cells. WT HuR and K182R mutant HuR also reduced the enhancement in the proliferation rate caused by TRIM21 overexpression in cells exposed to heat shock (**Fig. 2K**). Together, these findings demonstrated that TRIM21's ability to protect cells from heat shock-induced death is, at least partly, mediated by its degradation of HuR.

S100 and E101 residues of HuR are determinants of recognition by TRIM21

Heat shock induced the interaction between HuR and TRIM21 suggesting the presence of specific determinants of TRIM21 binding in HuR which might be post-translationally modified in response to heat shock. We adopted an unbiased approach to delineate the determinants of HuR interaction with TRIM21 under heat shock. His-tagged versions of various deletion mutants, consisting of different domains of the HuR protein, were constructed (**Fig. 3A**). When expressed in cells exposed to heat shock, only WT HuR and RRM1-2 showed degradation, indicating that the region of HuR interacting with TRIM21 was localized in RRM1-2 (**Fig. 3B**). Interestingly, RRM2-3, which still contained the K182 residue, did not show degradation under heat shock, suggesting that residues necessary for substrate recognition by TRIM2 were present in RRM1 or in the linker region. Also, only WT HuR and HuR RRM1-2 interacted with TRIM21, further indicating that RRM1-2 contained the residues crucial for recognition of HuR by TRIM21 (**Fig. 3C**).

We then adopted molecular dynamics (MD) simulation to identify the putative contact points between HuR and TRIM21. The MD simulation was performed with HuR RRM1-2 (PDB: 4EGL) and the PRYSPRY domain of TRIM21 (PDB: 2IWG), that has been shown to be responsible for substrate binding[29]. The simulation showed a rapid reduction and subsequent stabilization of the solvent accessible surface area (SASA) of the system indicating interaction between the two molecules (**Suppl. Fig. 5A**). The contact area was around 30 nm^2 and remained nearly constant throughout the length of the simulation post binding. The interaction was also energetically stable, being of the order of 10^3 kJ/mol and was mostly electrostatic (**Suppl. Fig. 5B**). The putative contact surface between HuR and TRIM21 showed two regions of HuR, between 98-106 amino acids and between 111-119 amino acids. Among these residues, the highest probability of contact was obtained for two amino acids, S100 and E101, located in the linker region between RRMs 1 and 2 (**Fig. 3D**). Another two amino acids, R115 and T116, also showed

interaction with TRIM21 residues but with lower probability. The molecular distance between S100 and K182, the site of TRIM21-mediated ubiquitination, was estimated to be 24.19 Å, whereas the distance between R115 and K182 was 19.22 Å (**Fig. 3E**). However, K182 and S100 are located on the same face of HuR, whereas R115 is located on the opposite face. The MD simulation results allowed the molecular docking of HuR RRM1-2 and TRIM21 PRYSPRY domains, showing a close contact between S100 residue of HuR and TRIM21 (**Fig. 3F**). The MD simulation and molecular docking results suggested S100 and E101 residues as the possible primary determinants of interaction between HuR and TRIM21.

S100 and E101 residues of HuR are required for TRIM21 binding and degradation of HuR under heat shock

The S100 and E101 residues of HuR were mutated to generate HuR S100A and E101A mutants and a S100A/E101A double mutant (**Fig. 4A**). All the three mutant HuR proteins were found to be refractory to heat shock-induced degradation while WT HuR was degraded efficiently (**Fig. 4B**). TRIM21 failed to interact with either of the single mutants or the double mutant, while it interacted efficiently with WT HuR (**Fig. 4C**). The S100A/E101A double mutant HuR also showed reduced ubiquitination compared to WT HuR under heat shock, (**Fig. 4D**). This demonstrated S100 and E101 residues as necessary for the heat shock-induced ubiquitination and degradation of HuR by TRIM21.

We checked the effect of the HuR S100A/E101A mutant on cell viability and apoptosis after exposure to heat shock. Overexpression of the HuR S100A/E101A double mutant significantly reversed the enhancement of cell viability and reduction in caspase activity observed upon TRIM21 overexpression both in cells exposed to 37°C and 43°C (**Fig. 4E, left top and bottom panels**). Similarly, overexpression of the HuR S100A/E101A mutant reversed the reduction in apoptosis of heat-stressed cells upon TRIM21 overexpression (**Fig. 4E, right top and bottom panels and Suppl. Fig 6**). The HuR double mutant also significantly reduced the enhanced proliferation of cells overexpressing TRIM21 during the 72 h period post exposure to heat shock (**Fig. 4F**). Therefore, the degradation-resistant S100A/E101A double mutant HuR could counteract TRIM21's ability to ensure cell survival and proliferation under heat shock.

We also tested whether the R115 and T116 residues were required for degradation of HuR and interaction with TRIM21. A R115A/T116A double mutant HuR showed degradation similar to WT HuR upon exposure to heat shock (**Suppl. Fig. 7A**). Also the R115A/T116A double mutant showed interaction with TRIM21 in cells exposed to heat shock (**Suppl. Fig. 7B**). Therefore, the R115 and T116A residues did not determine the interaction between HuR and TRIM21 and did not contribute to HuR degradation under heat shock.

Finally, we determined the effect of the S100A/E101A mutant on the mRNA levels of some of the post-transcriptional targets of HuR which are related to cell proliferation, apoptosis and stress responses. qRT-PCR for specific HuR target mRNAs showed that these mRNA levels were strongly reduced in WT HuR-overexpressing cells exposed to 43 °C, whereas overexpression of HuR S100A/E101A double mutant restored these mRNAs to nearly normal levels (**Fig. 4G**). Also, HuR S100A/E100A double mutant retained the ability to interact with these mRNAs (**Suppl. Fig. 8**). This indicated that the degradation resistant HuR

double mutant protein could bind with and stabilize the HuR target mRNAs which are otherwise destabilized in heat-stressed cells.

Phosphorylation of S100 is required for TRIM21 binding and degradation of HuR under heat shock

As phosphorylation of HuR have been shown to influence its sub-cellular localization and mRNA-binding ability under different stress conditions[24,30], we investigated whether S100 was phosphorylated in response to heat shock. WT HuR showed high level of serine phosphorylation in heat stressed cells whereas the S100A mutant showed strongly reduced serine phosphorylation, demonstrating S100 as a target for phosphorylation under heat shock (**Fig. 5A**). A phosphomimetic S100D mutant was degraded in cells even at 37°C (**Fig. 5B**). However, knockdown of TRIM21 prevented the degradation of HuR S100D mutant in the absence of heat shock (**Fig. 5C**). TRIM21 also efficiently interacted with the HuR S100D mutant both in absence and presence of heat shock, whereas it interacted efficiently with WT HuR only upon exposure to heat shock (**Fig. 5D**). Together, these data indicated that the phosphorylation of S100 was responsible for recognition of HuR by TRIM21 and subsequent degradation. We also investigated the effect of the S100D mutant on cell viability and apoptosis in response to heat shock. Overexpression of WT HuR reduced cell viability and enhanced caspase activity in heat-stressed cells, as observed before, whereas overexpression of the S100D mutant showed the opposite effect (**Fig. 5 E and F**). Therefore, the rapid degradation of the HuR S100D mutant provided the same survival advantage to the cells caused by TRIM21-mediated degradation of HuR under heat shock.

AKT1 phosphorylates S100 leading to TRIM21-mediated degradation of HuR under heat shock

We then proceeded to identify the kinase phosphorylating S100 of HuR in response to heat shock. S100 is part of a kinase substrate motif RXXS/T (**R97**PS**S100**) which was found to be conserved across vertebrates (**Fig. 6A**). One of the kinases with the substrate motif RXXS/T is AKT1, which plays a central role in mediating critical cellular responses including cell growth and survival[31,32]. AKT1 is also reported to be induced by heat shock and involved in suppression of heat shock-induced cell death[33,34]. Therefore we tested whether AKT1 might be the kinase phosphorylating HuR in response to heat shock. Treatment of cells with an Akt inhibitor prevented the degradation of HuR in heat stressed cells (**Fig. 6B**). siRNA-mediated knockdown of AKT1 also inhibited the degradation of HuR in response to heat shock **(Fig. 6C**). Exposure to 43°C increased the phosphorylation of AKT1 in a time-dependent manner, without increasing the level of AKT1, indicating the activation of AKT1 by heat shock (**Fig. 6D**). The Akt inhibitor prevented serine phosphorylation of HuR in response to heat shock (**Fig. 6E**). HuR also interacted with phosphoAKT1 in response to heat shock, which was abrogated by treatment with Akt inhibitor, suggesting that activated AKT1 interacted with HuR under heat shock (**Fig. 6F**). WT HuR interacted with phosphoAKT1 while the S100A mutant HuR failed to do so, showing S100 as the target for AKT1-mediated phosphorylation in response to heat shock (**Fig. 6G**).

As AKT1-mediated phosphorylation of S100 would be dependent on recognition of the substrate motif RXXS/T by AKT1, we disrupted this motif in HuR by mutating R97 to A. The HuR R97A mutant did not get degraded under heat shock, indicating the importance of the RXXS/T motif for substrate recognition by the kinase (**Fig. 6H**). The R97A mutant also did not undergo serine phosphorylation under heat shock, further demonstrating the requirement of the AKT1 recognition motif for serine phosphorylation of HuR under heat shock (**Fig. 6I**). Furthermore, the R97A mutant HuR failed to interact with phosphoAKT1 in response to heat shock (**Fig. 6J**). Together, these findings demonstrated the presence of S100 within a *bona fide* AKT1 substrate motif in HuR and AKT1 as the kinase phosphorylating S100 under heat shock.

Finally we checked whether AKT1-mediated phosphorylation of HuR was necessary for interaction of HuR with TRIM21 in response to heat shock. Treatment with the Akt inhibitor drastically reduced TRIM21 interaction with HuR in heat-stressed cells (**Fig. 6K**). siRNA-mediated knockdown of AKT1 also prevented the interaction of HuR with TRIM21 in response to heat shock (**Fig. 6L**). Finally, the R97A mutant also failed to interact with TRIM21 under heat shock whereas the WT HuR interacted efficiently (**Fig. 6M**). Together, these observations showed that AKT1-mediated phosphorylation of S100 in HuR allowed the binding of TRIM21 to HuR, leading to polyubiquitination of K182 and subsequent degradation of HuR in response to heat shock.

Discussion

Post-translational modification (PTM) has emerged as a central regulator of the abundance and functions of RBPs, thereby exerting important effects on the post-transcriptional gene regulatory networks governed by the RBPs[35]. Importantly, PTMs connect RBPs to multiple signal transduction pathways in cells, especially in response to stress signals, a connection that was hitherto mostly unexplored. This establishes the involvement of RBPs with the cellular signaling pathways, whose outcomes were previously considered to be mainly transcriptional in nature[36,37]. Abnormal PTM patterns of RBPs can therefore lead to the alteration of their physiological role and has been associated with the pathophysiology of various disease conditions [38–41].

PTMs of the RBP HuR have been shown to play especially important roles in regulating the abundance and function of HuR in response to various stimuli[24]. While HuR is predominantly nuclear in unstimulated cells, it undergoes nuclear-cytoplasmic translocation in response to various stimuli, including stress signals, inflammatory agonists and mitogens[20,42–44]. The nuclear-cytoplasmic translocation of HuR is often dependent on PTMs, especially phosphorylation, of specific residues in the HuR nuclear-cytoplasmic shuttling sequence (HNS) located in the hinge region [43,45–48]. Signal-dependent phosphorylation therefore acts as an important mechanism of regulation of HuR subcellular localization and RNA-binding activity.

Although changes in subcellular localization appears to be the major mode of regulation of HuR in response to multiple stimuli, controlled degradation often regulates HuR abundance and function in stress responses. Metabolic stress in cancer cells causes HuR translocation to the cytoplasm where it is

targeted by the ubiquitin E3 ligase βTrCP1 for degradation[49]. This is also connected to HuR phosphorylation, as phosphorylation at S318 by PKCα and phosphorylation at S304 by IKKα is required for nuclear-cytoplasmic shuttling and recognition of HuR by βTrCP1 respectively. Nuclear-cytoplasmic shuttling followed by degradation of HuR is also observed in response to genotoxic stress, mediated by the ubiquitin E3 ligase TRIM21[27,50]. HuR is also degraded by caspase-mediated cleavage in response to hypoxia and the apoptosis inducer staurosporine[51,52].

Regulated degradation of HuR is also induced in response to heat shock. Degradation of HuR under heat shock was also thought to be connected to phosphorylation of HuR, as the kinase CHK2, which phosphorylates HuR on S88, S100 and T118 upon H_2O_2 treatment, was found to protect HuR against degradation in heat-stressed cells[26]. HuR degradation under heat shock is also promoted by arginylation of HuR on D15, which was also required for its phosphorylation under heat shock[53]. Knockdown of the ring-finger domain containing E3 ubiquitin ligase Pirh2, which was found as an interacting partner of HuR, appeared to stabilize HuR protein under heat shock[54]. However, neither the ubiquitination of the K182 residue nor a direct interaction between Pirh2 and HuR under heat shock has been shown. Here we have shown that TRIM21 ubiquitinates K182 under heat shock, leading to its degradation. Moreover, TRIM21 enhances cell survival and reduces apoptosis in response to heat shock, an effect which is mediated by the degradation of HuR. TRIM21 overexpression also enhances cell proliferation and reduces apoptosis at physiological temperature, which conforms to reports of TRIM21's potential tumorigenic role[55–57]. Phosphorylation of S100 was found to be necessary for TRIM21 interaction with HuR and its subsequent degradation. Phosphorylation of S100, together with the presence of the adjacent E101 residue, possibly generates a negative patch on the flexible linker between RRMs 1 and 2 of HuR as a recognition site for TRIM21. Multiple amino acid residues in the linker and in the adjacent parts of RRMs 1 and 2 are sites of phosphorylation regulating different functions of HuR such as localization, RNA-binding and splicing regulation[24].

We have shown that the kinase AKT1 phosphorylates S100 and the AKT1-mediated phosphorylation of S100 is necessary for recognition by TRIM21 and degradation of HuR under heat shock. AKT1 or protein kinase B (PKB) acts as one of the most important mediators of cellular signal transduction pathways by phosphorylating a range of intracellular proteins[58]. AKT1 is known to regulate global mRNA translation by activating mammalian target of rapamycin (mTOR), which enhances translation initiation by phosphorylating ribosomal protein S6 and eIF4E-BPs[59]. However, the role of AKT1 in transcript-specific post-transcriptional control of gene expression is not known. By demonstrating AKT1 as causing the phosphorylation and consequent degradation of HuR, we have established a firm link between AKT1 and post-transcriptional regulation of gene expression in cells, especially in response to stress signals. AKT1-mediated phosphorylation of S100 in HuR generates the recognition site for TRIM21 which binds and ubiquitinates K182, leading to the proteasomal degradation of HuR, thereby constituting a heat-shock induced "phosphodegron" in HuR (Fig. 7). A phosphodegron is defined as a phosphorylated residue(s) on a protein that directly interacts with an interaction domain in an E3 ubiquitin ligase, thereby linking the substrate to the conjugation machinery[60]. The regulated degradation of HuR mediated by this

phosphodegron controls a crucial adaptive mechanism ensuring cell survival and homeostasis in response to thermal stress.

Materials And Methods

Plasmid Constructs

Wild type (WT) and deletion and point mutants of HuR coding region were cloned in mammalian expression vector pCDNA3.1 with Myc-His tag. TRIM21 expression construct and haemagluttinin (HA)-tagged ubiquitin expression consruct were gifts from Sunit. K. Singh, BHU, Varanasi, India. and S.N. Bhattacharyya, CSIR-IICB, Kolkata, India respectively.

Cell culture, treatment and transfection

MCF7 human breast carcinoma cells (ATCC HTB-22) grown in DMEM with 10% FBS (Thermo Fisher Scientific, Waltham, MA, USA) were exposed to heat shock at 43°C for 2 h. Cells were treated with 100 µg/ml cyclohexamide (Amresco, Cleveland, OH, USA) or 10 µM MG132 (Sigma Aldrich, St. Louis, MO, USA) for 1 h, or 10 µM Akt Inhibitor (Sigma Aldrich) for 2 h. Cells were transfected with plasmid vectors, siRNAs (siGENOME SMARTpool TRIM21 (Horizon Discovery, UK), or Invitrogen Silencer Select siRNA for Akt and SMARTpool non-targeting siRNA (Horizon Discovery) or Control siRNA (Sigma MissionsiRNA Universal Negative Control) using Lipofectamine2000 or Turbofect (Thermo Fisher) or peiRfect transfection reagent (BioBharati Life Sciences, India).

Immunoblotting

Lysates of MCF7 cells in S10 lysis buffer were resolved by SDS-PAGE, transferred to PVDF membrane (MilliporeSigma, Burlington, MA, USA), and immunoblotted with antibodies anti-HuR (Santa Cruz Biotechnology, Dallas, TX, USA), TRIM21, Ubiquitin, Myc (Cell Signaling Technology, Danvers, MA, USA), His (BioBharati LifeScience), AKT (ProteinTech), phosphoAkt (R&D Systems), phosphoSerine (Santa Cruz Biotechnology), non-immune IgG (BioBharati), HRP conjugated b-actin (Genscript, Piscataway, NJ, USA) and GAPDH (Santa Cruz Biotechnology) antibodies as primary antibodies. HRP conjugated anti-mouse or anti-rabbit (Cell Signaling Technologies) were used as secondary antibodies. Chemiluminescent signal was detected using FemtolucentPlus HRP substrate (Geno Biosciences, St. Louis, MO, USA).

Coimmunoprecipitation

Cells treated with MG132 and exposed to 43°C for 1h, were lysed with Pierce Direct IP Kit lysis buffer (Thermo Fisher). Lysates were immunoprecipitated with anti-HuR and anti-TRIM21 antibodies using

Pierce Direct IP Kit following manufacturer's protocol, followed by immunoblotting using specific antibodies.

Ni-NTA affinity pulldown assay

MCF7 cells overexpressing His-tagged WT or deletion or point mutant HuR proteins were lysed in NT2 buffer with 10 mM imidazole or NT2 buffer supplemented with 5mM NaF and 5mM Na_3VO_4 for phosphoserine and phoshoAkt pulldown assay. Lysates were incubated with Ni-NTA agarose beads (Qiagen, Germany) overnight at 4°C, washed multiple times with NT2 buffer containing 20 mM Imidazole, following which the proteins were eluted in SDS-PAGE gel-loading dye and resolved by SDS–PAGE followed by immunoblotting using appropriate antibodies.

Ubiquitination Assay

Cells co-transfected with HA-ubiquitin and His-tagged HuR WT treated with MG132 and exposed to 43°C were lysed in ubiquitination lysis buffer with 0.2 mM ATP and subjected to Ni-affinity pull down. The precipitates were washed in NT2 buffer with 20 mM imidazole, following which the precipitates were resolved by SDS-PAGE and immunoblotted with anti-ubiquitin and anti-His antibodies.

RNA-coprecipitation assay:

Cells lysed in NT2 buffer supplemented with 10 mM imidazole were subjected to a Ni-NTA pulldown assay as described earlier. After multiple washes, 20% of the beads were used for western blotting and RNA was isolated from the rest using RNAiso Plus reagent (Takara Bio, Japan). Reverse transcription was done with MMLV RT enzyme (Thermo Fisher) and qPCR was performed using target specific primers.

Quantitative PCR

Total cellular RNA was isolated using RNAiso Plus (Takara Bio). cDNA was synthesized using oligo(dT) primers by MMLV reverse transcriptase (Thermo Fisher). Gene specific primers were used for qPCR using Power SYBR Green reagent (Thermo Fisher), in StepOne plus real-time PCR system (Thermo Fisher). GAPDH mRNA level was used for normalization.

MD Simulation and Analysis:

The GROMOS 54A7[61] force field was used for molecular dynamic simulations. GROMACS[62] was used as the simulation engine and the water type used was SPC/E (simple point charge extended). The favorable 'pose' of the two proteins were computed using molecular docking of the two protein structures (as obtained from PDB) by HADDOCK[63]. The final MD run was carried out in conditions of NPT for a total time of 400 ns. PDB structures were visualized by Visual Molecular Dynamics (VMD)[64]. Contact between the two proteins was derived by the reduction in the total solvent accessible surface area (SASA)[65] and residues of contact were determined by checking the pairs of residues (in HuR *vs* TRIM21) that have their α-carbons within 1 nm of each other.

Cell viability and apoptosis assays

MCF7 cells transfected with plasmid construct or siRNA and subjected to 2 h of heat shock at 43°C post 48 h of transfection, were assayed for cell viability by MTT assay (Sigma Aldrich). Caspase 3/7 activity was measured by CaspaseGlo 3/7 assay (Promega, Madison, WI, USA). Apoptosis of cells was estimated by Annexin V/PI staining using AlexaFluor-488 Annexin V/Dead Apoptosis Kit (Thermo Fisher) followed by epifluorescence microscopy.

Morphology analysis

Cell spread area and perimeterwere determined. Phase contrast images of MCF7 cells transfected with TRIM21 expression vector or TRIM21 siRNA and exposed to 2 h of heat shock were captured using Olympus IX81 inverted microscope using Micromanager software. ImageJ (NIH, USA) software was used for cell spread area analysis. The cell spread areas and perimeters of 400 cells from three different biological repeats were calculated and the data was plotted using GraphPad Prism software.

Cell proliferation and colony formation assay

Cells transfected with plasmid constructs/siRNAs were exposed to 2 h of heat shock 48 hours after transfection and returned to 37°C. Cell proliferation was estimated by MTT assay (Sigma Aldrich) at different time points. For colony-forming assay, transfected MCF7 cells were exposed to heat shock following which they were seeded and allowed to form colonies for 14 days. Colonies were stained with crystal violet and CFUs (colony forming units) were counted.

Live Cell Imaging

Live cell confocal fluorescence time-lapse imaging was performed to measure HuR degradation. Cells were seeded in 35 mm glass bottom dishes (SPL Lifesciences, Korea) and transfected with construct expressing EGFP-tagged HuR WT protein. Post 24 h of transfection, time lapse videos were recorded over a period of 2 h in LSM 710 confocal microscope (Carl Zeiss) in an environmental chamber in 5% CO_2 and 37°C or 43 °C. GFP intensity of whole cell was measured using ZEN 2010 software (Carl Zeiss) and plotted against time.

Statistical analysis

All graphical data represent mean ± standard deviation of at least three independent biological replicates. Single, double and triple *, #, $, @, α, β, γ, δ signs signify p-values ≤ 0.05, ≤ 0.01 and ≤ 0.005 (paired two-tailed Student's t test or one-tailed Student's t test as applicable) between controls and samples respectively as indicated in the figures.

References

1. Milisav I, Poljšak B, Ribarič S. Reduced risk of apoptosis: mechanisms of stress responses. Apoptosis 2017; **22**: 265–283.
2. Vihervaara A, Duarte FM, Lis JT. Molecular mechanisms driving transcriptional stress responses. Nat. Rev. Genet. 2018; **19**: 385–397.
3. Pizzinga M, Harvey RF, Garland GD, Mordue R, Dezi V, Ramakrishna M *et al.* The cell stress response: extreme times call for post-transcriptional measures. John Wiley & Sons, Ltd, 2020.
4. Gebauer F, Schwarzl T, Valcárcel J, Hentze MW. RNA-binding proteins in human genetic disease. Nat Rev Genet 2020; **22**: 185–198.
5. Nag S, Goswami B, Das Mandal S, Ray PS. Cooperation and competition by RNA-binding proteins in cancer. Semin Cancer Biol 2022. doi:10.1016/J.SEMCANCER.2022.02.023.
6. Yao RW, Wang Y, Chen LL. Cellular functions of long noncoding RNAs. Nat Cell Biol 2019; **21**: 542–551.
7. Backlund M, Stein F, Rettel M, Schwarzl T, Perez-Perri JI, Brosig A *et al.* Plasticity of nuclear and cytoplasmic stress responses of RNA-binding proteins. Nucleic Acids Res 2020; **48**: 4725–4740.
8. Richter K, Haslbeck M, Buchner J. The Heat Shock Response: Life on the Verge of Death. Mol. Cell. 2010; **40**: 253–266.
9. Lindquist S. The heat-shock response. Annu. Rev. Biochem. 1986; **55**: 1151–1191.
10. Gasch AP, Spellman PT, Kao CM, Carmel-Harel O, Eisen MB, Storz G *et al.* Genomic expression programs in the response of yeast cells to environmental changes. Mol Biol Cell 2000; **11**: 4241–4257.
11. Stephanou A, Latchman DS. Transcriptional Modulation of Heat-Shock Protein Gene Expression. *Biochem Res Int* 2011; **2011**. doi:10.1155/2011/238601.
12. Paszek A, Kardyńska M, Bagnall J, Śmieja J, Spiller DG, Widłak P *et al.* Heat shock response regulates stimulus-specificity and sensitivity of the pro-inflammatory NF-κB signalling. Cell Commun Signal 2020; **18**. doi:10.1186/s12964-020-00583-0.
13. Takayama S, Reed JC, Homma S. Heat-shock proteins as regulators of apoptosis. Oncogene 2003 2256 2003; **22**: 9041–9047.
14. Spriggs KA, Bushell M, Willis AE. Translational Regulation of Gene Expression during Conditions of Cell Stress. Mol Cell, 2010.
15. Shalgi R, Hurt JA, Krykbaeva I, Taipale M, Lindquist S, Burge CB. Widespread Regulation of Translation by Elongation Pausing in Heat Shock. Mol Cell 2013; **49**: 439–452.
16. Harvey R, Dezi V, Pizzinga M, Willis AE. Post-transcriptional control of gene expression following stress: the role of RNA-binding proteins. Biochem Soc Trans 2017; **45**: 1007–1014.
17. Srikantan S, Abdelmohsen K, Lee EK, Tominaga K, Subaran SS, Kuwano Y *et al.* Translational control of TOP2A influences doxorubicin efficacy. Mol Cell Biol 2011; **31**: 3790–801.
18. Abdelmohsen K, Pullmann R, Lal A, Kim HH, Galban S, Yang X *et al.* Phosphorylation of HuR by Chk2 regulates SIRT1 expression. Mol Cell 2007; **25**: 543–557.

19. Galbán S, Kuwano Y, Pullmann R, Martindale JL, Kim HH, Lal A *et al.* RNA-Binding Proteins HuR and PTB Promote the Translation of Hypoxia-Inducible Factor 1α. Mol Cell Biol 2008; **28**: 93–107.
20. Poria DK, Guha A, Nandi I, Ray PS. RNA-binding protein HuR sequesters microRNA-21 to prevent translation repression of proinflammatory tumor suppressor gene programmed cell death 4. Oncogene 2016; **35**: 1703–1715.
21. Bhattacharyya SN, Habermacher R, Martine U, Closs EI, Filipowicz W. Relief of microRNA-mediated translational repression in human cells subjected to stress. Cell 2006; **125**: 1111–24.
22. Gallouzi IE, Brennan CM, Stenberg MG, Swanson MS, Eversole A, Maizels N *et al.* HuR binding to cytoplasmic mRNA is perturbed by heat shock. Proc Natl Acad Sci U S A 2000; **97**: 3073.
23. Srikantan S, Gorospe M. HuR function in disease. Front. Biosci. 2012; **17**: 189–205.
24. Grammatikakis I, Abdelmohsen K, Gorospe M. Posttranslational control of HuR function. Wiley Interdiscip Rev RNA 2017; **8**: e1372.
25. Gallouzi IE, Brennan CM, Steitz JA. Protein ligands mediate the CRM1-dependent export of HuR in response to heat shock. RNA 2001; **7**: 1348–61.
26. Abdelmohsen K, Srikantan S, Yang X, Lal A, Kim HH, Kuwano Y *et al.* Ubiquitin-mediated proteolysis of HuR by heat shock. EMBO J 2009; **28**: 1271–82.
27. Guha A, Ahuja D, Das Mandal S, Parasar B, Deyasi K, Roy D *et al.* Integrated Regulation of HuR by Translation Repression and Protein Degradation Determines Pulsatile Expression of p53 Under DNA Damage. iScience 2019; **15**: 342–359.
28. Guha A, Nag S, Ray PS. Negative feedback regulation by HuR controls TRIM21 expression and function in response to UV radiation. Sci Reports 2020 101 2020; **10**: 1–14.
29. James LC, Keeble AH, Khan Z, Rhodes DA, Trowsdale J. Structural basis for PRYSPRY-mediated tripartite motif (TRIM) protein function. Proc Natl Acad Sci U S A 2007; **104**: 6200–6205.
30. Eberhardt W, Doller A, Pfeilschifter J. Regulation of the mRNA-binding protein HuR by posttranslational modification: spotlight on phosphorylation. Curr Protein Pept Sci 2012; **13**: 380–390.
31. Obata T, Yaffe MB, Leparc GG, Piro ET, Maegawa H, Kashiwagi A *et al.* Peptide and Protein Library Screening Defines Optimal Substrate Motifs for AKT/PKB. J Biol Chem 2000; **275**: 36108–36115.
32. Nicholson KM, Anderson NG. The protein kinase B/Akt signalling pathway in human malignancy. Cell Signal 2002; **14**: 381–395.
33. Shaw M, Cohen P, Alessi DR. The activation of protein kinase B by H2O2 or heat shock is mediated by phosphoinositide 3-kinase and not by mitogen-activated protein kinase-activated protein kinase-2. Biochem J 1998; **336**: 241.
34. Bang OS, Ha BG, Park EK, Kang SS. Activation of Akt is induced by heat shock and involved in suppression of heat-shock-induced apoptosis of NIH3T3 cells. Biochem Biophys Res Commun 2000; **278**: 306–311.

35. Velázquez-Cruz A, Baños-Jaime B, Díaz-Quintana A, De la Rosa MA, Díaz-Moreno I. Post-translational Control of RNA-Binding Proteins and Disease-Related Dysregulation. Front Mol Biosci 2021; **8**: 234.
36. Sugiura R, Satoh R, Ishiwata S, Umeda N, Kita A. Role of RNA-Binding Proteins in MAPK Signal Transduction Pathway. J Signal Transduct 2011; **2011**: 1–8.
37. Venigalla RKC, Turner M. RNA-binding proteins as a point of convergence of the PI3K and p38 MAPK pathways. Front Immunol 2012; **3**: 398.
38. Qamar S, Wang GZ, Randle SJ, Ruggeri FS, Varela JA, Lin JQ *et al.* FUS Phase Separation Is Modulated by a Molecular Chaperone and Methylation of Arginine Cation-π Interactions. Cell 2018; **173**: 720–734.e15.
39. Gongol B, Marin T, Zhang J, Wang SC, Sun W, He M *et al.* Shear stress regulation of miR-93 and miR-484 maturation through nucleolin. Proc Natl Acad Sci U S A 2019; **116**: 12974–12979.
40. Doller A, Winkler C, Azrilian I, Schulz S, Hartmann S, Pfeilschifter J *et al.* High-constitutive HuR phosphorylation at Ser 318 by PKCd propagates tumor relevant functions in colon carcinoma cells. Carcinogenesis 2011; **32**: 676–685.
41. Tiedje C, Ronkina N, Tehrani M, Dhamija S, Laass K, Holtmann H *et al.* The p38/MK2-Driven Exchange between Tristetraprolin and HuR Regulates AU-Rich Element-Dependent Translation. PLoS Genet 2012; **8**: e1002977.
42. Mazan-Mamczarz K, Galbán S, López de Silanes I, Martindale JL, Atasoy U, Keene JD *et al.* RNA-binding protein HuR enhances p53 translation in response to ultraviolet light irradiation. Proc Natl Acad Sci U S A 2003; **100**: 8354–9.
43. Lafarga V, Cuadrado A, Lopez de Silanes I, Bengoechea R, Fernandez-Capetillo O, Nebreda AR. p38 Mitogen-Activated Protein Kinase- and HuR-Dependent Stabilization of p21 Cip1 mRNA Mediates the G 1 /S Checkpoint. Mol Cell Biol 2009; **29**: 4341–4351.
44. Atasoy U, Watson J, Patel D, Keene JD. ELAV protein HuA (HuR) can redistribute between nucleus and cytoplasm and is upregulated during serum stimulation and T cell activation. J Cell Sci 1998; **111 (Pt 21)**: 3145–3156.
45. Doller A, Schlepckow K, Schwalbe H, Pfeilschifter J, Eberhardt W. Tandem Phosphorylation of Serines 221 and 318 by Protein Kinase Cδ Coordinates mRNA Binding and Nucleocytoplasmic Shuttling of HuR. Mol Cell Biol 2010; **30**: 1397–1410.
46. Kim HH, Abdelmohsen K, Lal A, Pullmann R, Yang X, Galban S *et al.* Nuclear HuR accumulation through phosphorylation by Cdk1. Genes Dev 2008; **22**: 1804–1815.
47. Filippova N, Yang X, King P, Nabors LB. Phosphoregulation of the RNA-binding protein Hu antigen R (HuR) by Cdk5 affects centrosome function. J Biol Chem 2012; **287**: 32277–32287.
48. Yoon JH, Abdelmohsen K, Srikantan S, Guo R, Yang X, Martindale JL *et al.* Tyrosine phosphorylation of HuR by JAK3 triggers dissociation and degradation of HuR target mRNAs. Nucleic Acids Res 2014; **42**: 1196–1208.
49. Chu P-C, Chuang H-C, Kulp SK, Chen C-S. The mRNA-stabilizing factor HuR protein is targeted by β-TrCP protein for degradation in response to glycolysis inhibition. J Biol Chem 2012; **287**: 43639–50.

50. Ahuja D, Goyal A, Ray PS. Interplay between RNA-binding protein HuR and microRNA-125b regulates p53 mRNA translation in response to genotoxic stress. RNA Biol 2016; **13**: 1152–1165.
51. Mazroui R, Di Marco S, Clair E, Von Roretz C, Tenenbaum SA, Keene JD *et al.* Caspase-mediated cleavage of HuR in the cytoplasm contributes to pp32/PHAP-I regulation of apoptosis. J Cell Biol 2008; **180**: 113–127.
52. Talwar S, Jin J, Carroll B, Liu A, Gillespie MB, Palanisamy V. Caspase-mediated cleavage of RNA-binding protein HuR regulates c-Myc protein expression after hypoxic stress. J Biol Chem 2011; **286**: 32333–43.
53. Deka K, Saha S. Heat stress induced arginylation of HuR promotes alternative polyadenylation of Hsp70.3 by regulating HuR stability and RNA binding. Cell Death Differ 2020 282 2020; **28**: 730–747.
54. Daks A, Petukhov A, Fedorova O, Shuvalov O, Kizenko A, Tananykina E *et al.* The RNA-binding protein HuR is a novel target of Pirh2 E3 ubiquitin ligase. Cell Death Dis 2021 126 2021; **12**: 1–14.
55. Zhao Z, Wang Y, Yun D, Huang Q, Meng D, Li Q *et al.* TRIM21 overexpression promotes tumor progression by regulating cell proliferation, cell migration and cell senescence in human glioma. Am J Cancer Res 2020; **10**: 114.
56. Alomari M. TRIM21 – A potential novel therapeutic target in cancer. Pharmacol Res 2021; **165**: 105443.
57. Zhu X, Xue J, Jiang X, Gong Y, Gao C, Cao T *et al.* TRIM21 suppresses CHK1 activation by preferentially targeting CLASPIN for K63-linked ubiquitination. Nucleic Acids Res 2022; **50**: 1517–1530.
58. Manning BD, Cantley LC. AKT/PKB Signaling: Navigating Downstream. Cell 2007; **129**: 1261–1274.
59. Hay N, Sonenberg N. Upstream and downstream of mTOR. Genes Dev 2004; **18**: 1926–1945.
60. Ang XL, Harper JW. SCF-mediated protein degradation and cell cycle control. Oncogene 2005; **24**: 2860–2870.
61. Schmid N, Eichenberger AP, Choutko A, Riniker S, Winger M, Mark AE *et al.* Definition and testing of the GROMOS force-field versions 54A7 and 54B7. Eur Biophys J 2011. doi:10.1007/s00249-011-0700-9.
62. Van Der Spoel D, Lindahl E, Hess B, Groenhof G, Mark AE, Berendsen HJC. GROMACS: Fast, flexible, and free. J. Comput. Chem. 2005. doi:10.1002/jcc.20291.
63. Van Zundert GCP, Rodrigues JPGLM, Trellet M, Schmitz C, Kastritis PL, Karaca E *et al.* The HADDOCK2.2 Web Server: User-Friendly Integrative Modeling of Biomolecular Complexes. J Mol Biol 2016; **428**: 720–725.
64. Humphrey W, Dalke A, Schulten K. VMD: Visual molecular dynamics. J Mol Graph 1996; **14**: 33–38.
65. Lee B, Richards FM. The interpretation of protein structures: Estimation of static accessibility. J Mol Biol 1971; **55**: 379-IN4.

Declarations

Acknowledgements

We thank S. K. Singh (BHU, Varanasi, India) and S. N. Bhattacharyya (CSIR-IICB, Kolkata, India) for providing reagents. We thank Neelanjana Sengupta (IISER Kolkata, India) and her lab members for help with MD simulation and Swarang Pundalik and Ravi Kumar (IISER Kolkata) for reagents.

Funding

This work was supported by a Wellcome Trust-DBT India Alliance intermediate fellowship (WT500139/Z/09/Z) and Science and Engineering Research Board (SERB) Extramural research grant (EMR/2016/003525) to P.S.R.

Author contributions

A.G, S.N and P.S.R conceived the project, S.N and S.R performed experiments, S.N, S.R. and P.S.R analyzed data, P.S.R and S.N wrote the manuscript, P.S.R obtained funding and supervised the project.

Competing interests

The authors declare no conflict of interests.

Figures

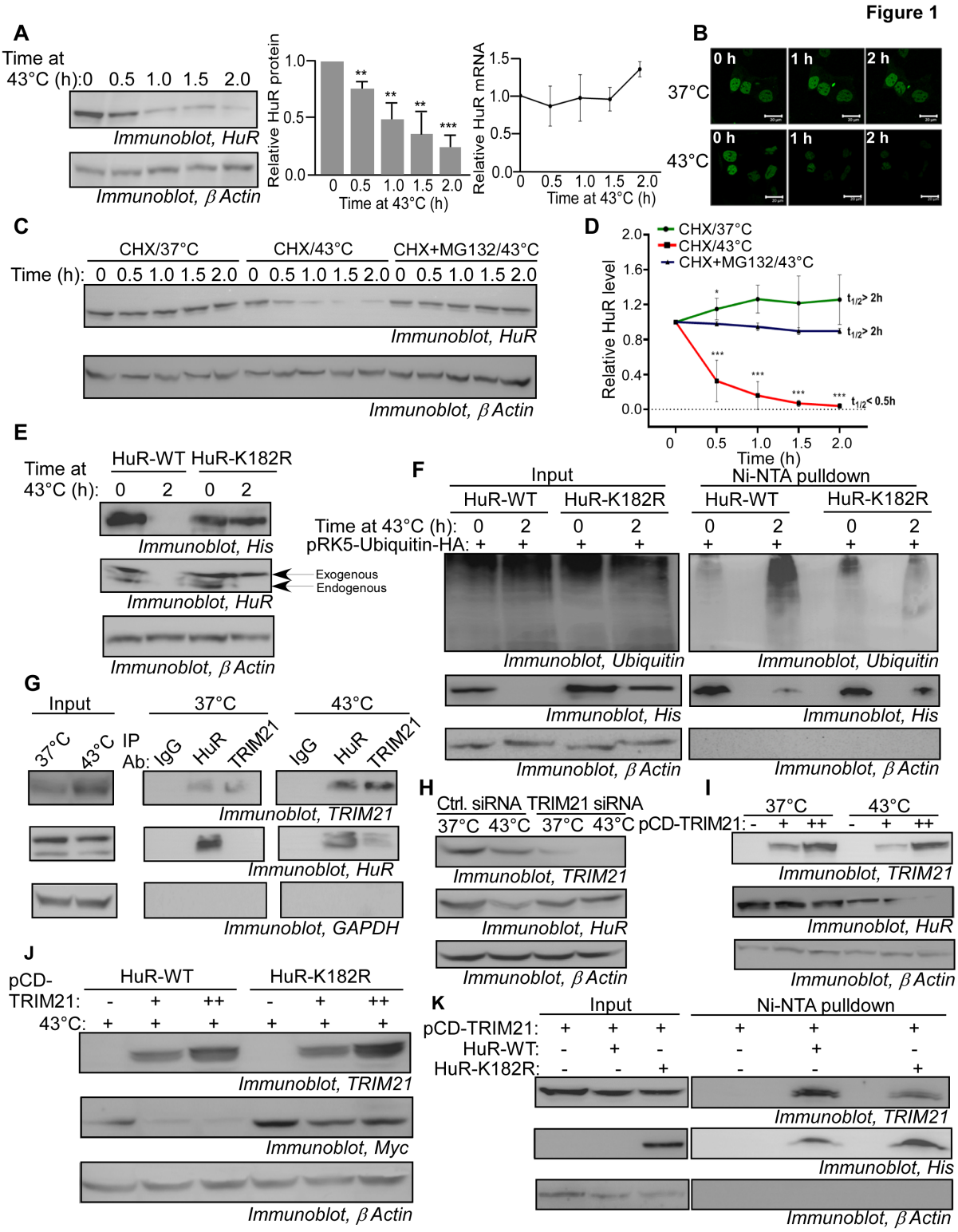

Figure 1

The E3 ubiquitin ligase TRIM21 mediates the degradation of HuR in response to heat shock. (**A**) Immunoblot of lysates of MCF7 cells either unexposed or exposed to heat shock at 43°C in presence of 10% FBS and collected at the indicated time points, probed with HuR and β Actin antibodies. Quantification of relative HuR protein levels (normalized to β Actin protein levels) with HuR protein level in cells not exposed to heat shock taken as 1. Quantification of relative fold change in HuR mRNA levels of

MCF7 cells exposed to heat shock for the indicated time points with HuR mRNA level in cells not exposed to heat shock taken as 1. GAPDH mRNA level was used to normalize HuR mRNA levels **signifies a p value ≤ 0.01, ***signifies a p value ≤ 0.005. The data represent mean ± SD values from three independent experiments. (**B**) Fluorescent microscopic images of MCF7 cells expressing HuR WT-EGFP fusion protein imaged live for a period of 2 h at 37°C or 43°C. Images were obtained by confocal microscopy at 60X magnification at the indicated time points. (**C**) Immunoblot of lysates of MCF7 cells treated with CHX at 37°C or with CHX at 43°C or with both CHX and MG132 at 43°C and collected at the indicated time points and probed with antibodies against HuR and β Actin. (**D**) Quantification of relative HuR protein levels (normalized to β Actin) plotted against indicated time points for each experimental setup in (C). Data represent mean ± SD values from three independent experiments. * signifies p value ≤ 0.05, *** signifies p value ≤ 0.005 (paired two-tailed t-test). (**E**) Immunoblot of lysates of MCF7 cells transfected with either pCDNA3-HuR WT_Myc-His (HuR-WT) or pCDNA3-HuR-K182R_Myc-His (HuR-K182R) and exposed to heat shock for 2 h, post 24 h of transfection. The blot was probed with His, HuR and β Actin antibodies. (**F**) MCF7 cells expressing HA-tagged Ubiquitin and His-tagged HuR-WT or HuR-K182R mutant proteins were treated with MG132 and subsequently exposed or unexposed to heat shock for 1 h. His-tagged proteins were precipitated from the cell lysate by Ni-NTA affinity pulldown and the precipitates probed with ubiquitin, His and β Actin antibodies. The left panels represent the input lysates probed with the same antibodies. (**G**) Lysates of MCF7 cells co-transfected with HuR-WT and TRIM21 expressing constructs, treated with MG132 and exposed to 37°C or 43°C, were immunoprecipitated with non-immune IgG or HuR or TRIM21 antibodies and the immunoprecipitates probed with TRIM21, HuR and GAPDH antibodies. Left panels represent the input lysates probed with the same antibodies. (**H**) Lysates of MCF7 cells transfected with either control siRNA or TRIM21 siRNA and either exposed or unexposed to heat shock for 2 h, post 24 h of siRNA transfection, immunoblotted with TRIM21, HuR and β Actin antibodies. (**I**) Lysates of MCF7 cells transfected with two increasing doses of TRIM21-expressing construct and either exposed or not exposed to heat shock for 2 h, post 48 h of transfection, immunoblotted with TRIM21, HuR and β Actin antibodies. (**J**) Lysates of MCF7 cells co-transfected with TRIM21, Myc-His-tagged HuR-WT or HuR-K182R-expressing constructs and exposed to heat shock for 2h, immunoblotted with TRIM21, Myc and β Actin antibodies. (**K**) Lysates of MCF7 cells co-transfected with TRIM21 and His tagged HuR-WT or HuR-K182R-expressing constructs, treated with MG132 and exposed to 1 h of heat shock, were subjected to Ni-NTA affinity pulldown of His-tagged proteins. The precipitates were immunoblotted with TRIM21, His and β Actin antibodies. Left panels represent the input lysates probed with the same antibodies.

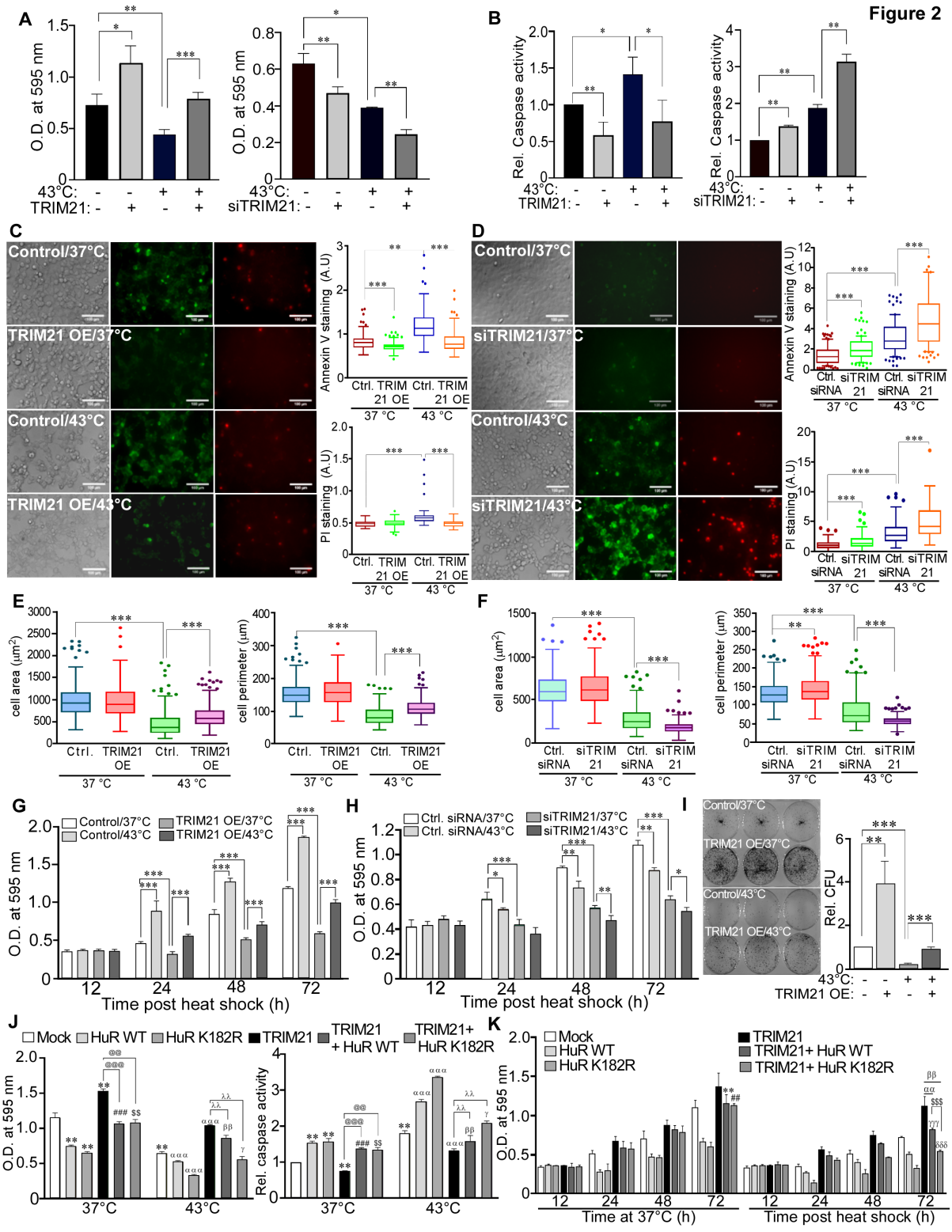

Figure 2

TRIM21 protects cells from heat shock-induced cell death by degrading HuR. (**A**) MCF7 cells transfected either with TRIM21-expressing plasmid or siRNA against TRIM21 (siTRIM21) were unexposed or exposed to heat shock at 43°C for 2 h. MTT assay of cells was performed post 2 h of heat shock and optical density (OD) at 595 nm was measured. Data represent mean ± SD values from three independent experiments. * signifies p value ≤ 0.05, ** signifies p value ≤ 0.01 and *** signifies p value ≤ 0.005

(paired two-tailed t-test). (**B**) MCF7 cells transfected either with TRIM21-expressing plasmid or siTRIM21 were unexposed or exposed to heat shock at 43°C for 2 h. Caspase 3/7 activity assay with a luminescent substrate was performed immediately post 2 h of heat shock. Relative light unit (RLU) values of each sample are expressed as fold change from that of cells transfected either with empty vector or control siRNA at 37°C, taken as 1. Data represents mean ± SD values from three independent experiments.* signifies p value ≤ 0.05, ** signifies p value ≤ 0.01 (paired two-tailed t-test). (**C**) MCF7 cells transfected either with empty vector (control) or TRIM21-expressing plasmid (TRIM21 OE) were unexposed or exposed to heat shock at 43°C for 2 h, post 48 h of transfection. Cells were then stained with AnnexinV-AlexaFluor 488 and propidium iodide to detect apoptosis by fluorescent microscopy. Quantification of fluorescent intensity per cell of Annexin V and propidium iodide staining was determined and is depicted in the box plots in the right panel. Data represent mean ± SD values of fluorescent intensity/cell from 100 cells that were randomly selected from each treatment. ** signifies p value ≤ 0.01, ***signifies p value ≤ 0.005 (paired two-tailed t-test). (**D**) MCF7 cells transfected either with control siRNA or siTRIM21 were unexposed or exposed to heat shock at 43°C for 2 h, post 48 h of transfection. Cells were then processed and data represented as in (C). ***signifies a p value ≤ 0.005 (paired two-tailed t-test). (**E**) MCF7 cells transfected either with empty vector (control) or TRIM21-expressing plasmid (TRIM21 OE) were unexposed or exposed to heat shock at 43°C for 2 h, post 48 h of transfection. Cells were then imaged at 10X in phase contrast microscope and projected cell areas and cell perimeters were determined using ImageJ software. Data represent mean ± SD values from 400 cells randomly selected from each experimental setup in individual biological repeats. *** signifies p value ≤ 0.005 (paired two-tailed t-test). (**F**) MCF7 cells transfected either with control siRNA or siTRIM21 were unexposed or exposed to heat shock at 43°C for 2 h, post 48 h of transfection. Data was then collected and analyzed as in (E). ** signifies p value ≤ 0.01, *** signifies p value ≤ 0.005 (paired two-tailed t-test). (**G**) MCF7 cells transfected either with empty vector (control) or TRIM21-expressing plasmid (TRIM21 OE) were unexposed or exposed to heat shock at 43°C for 2 h, post 48 h of transfection, following which they were allowed to grow at 37°C for 72 h. Cells were collected at indicated time points and MTT assay was performed. Data represent mean ± SD values from three independent experiments. *** signifies p value ≤ 0.005 (paired two-tailed t-test). (**H**) MCF7 cells transfected either with control siRNA or siTRIM21 were unexposed or exposed to heat shock at 43°C for 2 h, post 48 h of transfection, following which they were allowed to grow at 37°C for 72 h. Cells were collected at indicated time points and MTT assay was performed. * signifies p value ≤ 0.05, ** signifies p value ≤ 0.01 and ***signifies p value ≤ 0.005 (paired two-tailed t-test). (**I**) MCF7 cells transfected either with empty vector (control) or TRIM21-expressing plasmid (TRIM21 OE) were unexposed or exposed to heat shock at 43°C for 2 h, post 48 h of transfection, following which 10^3 cells were seeded and allowed to form colonies at 37 °C. After 14 days, colonies were counted by crystal violet staining (left panel). Relative colony forming unit (CFU) values from 3 independent experiments were plotted (right panel). ** signifies p value ≤ 0.01 and *** signifies p value ≤ 0.005 (paired two-tailed t-test). (**J**) MCF7 cells transfected with either empty vector (Mock), HuR WT, HuR K182R and TRIM21-expressing plasmids, individually or in combination, were either unexposed or exposed to heat shock at 43°C 2h. MTT assay was performed immediately post 2 h of heat shock (left panel). Caspase 3/7 activity assay with a luminescent substrate was performed immediately post 2 h of heat

shock. RLU values of each sample are expressed as fold change from that of mock-transfected cells at 37°C, taken as 1 (right panel). Data for both panels represent mean ± SD values from three independent experiments. ∗∗ represent significant difference (p-value ≤0.01) from mock-transfected cells at 37°C, ### represents significant difference (p-value ≤0.005) with respect to HuR WT expressing cells at 37°C, $$ represents significant difference (p-value ≤0.01) with respect to HuR K182R expressing cells at 37°C, @@ and @@@ represent significant difference (p-value ≤0.01 and ≤0.005 respectively) with respect to TRIM21 expressing cells at 37°C. ααα represents significant difference (p-value ≤0.005) with respect to mock transfected cells at 43°C, ββ represents significant difference (p-value ≤0.01) with respect to HuR WT expressing cells at 43°C, γ represents significant difference (p-value ≤ 0.05) with respect to HuR K182R expressing cells at 43°C and λλ represents significant difference (p-value ≤0.01) with respect to TRIM21 expressing cells at 43°C (paired two-tailed t-test). (**K**) MCF7 cells transfected with either empty vector (Mock), HuR WT, HuR K182R and TRIM21-expressing plasmids, individually or in combination, were either unexposed or exposed to heat shock at 43°C for 2 h following which they were allowed to grow at 37°C for 72 h. MTT assay was performed at the indicated time points. Data represent mean ± SD values from three independent experiments. ∗∗ represent significant difference (p-value ≤0.01) from HuR WT expressing cells at 37°C, ## represents significant difference (p-value ≤0.01) from HuR K182R expressing cells at 37°C, αα represents significant difference (p-value ≤0.01) of TRIM21 and HuR WT co-transfected cells with respect to TRIM21 transfected cells at 43°C, ββ represents significant difference (p-value ≤0.01) between TRIM21 and HuR K182R co-expressing cells with respect to TRIM21 expressing cells at 43°C, γγγ represents significant difference (p-value ≤ 0.001) between TRIM21 and HuR WT co-transfected cells with respect to HuR WT expressing cells at 43°C, δδδ represents significant difference (p-value ≤ 0.005) between TRIM21 and HuR K182R expressing cells and HuR K182R at 43°C, and $$$ represents significant difference (p-value ≤0.005) between TRIM21 and HuR WT co-expressing cells and TRIM21 and HuR K182R expressing cells at 43°C (paired two-tailed t-test).

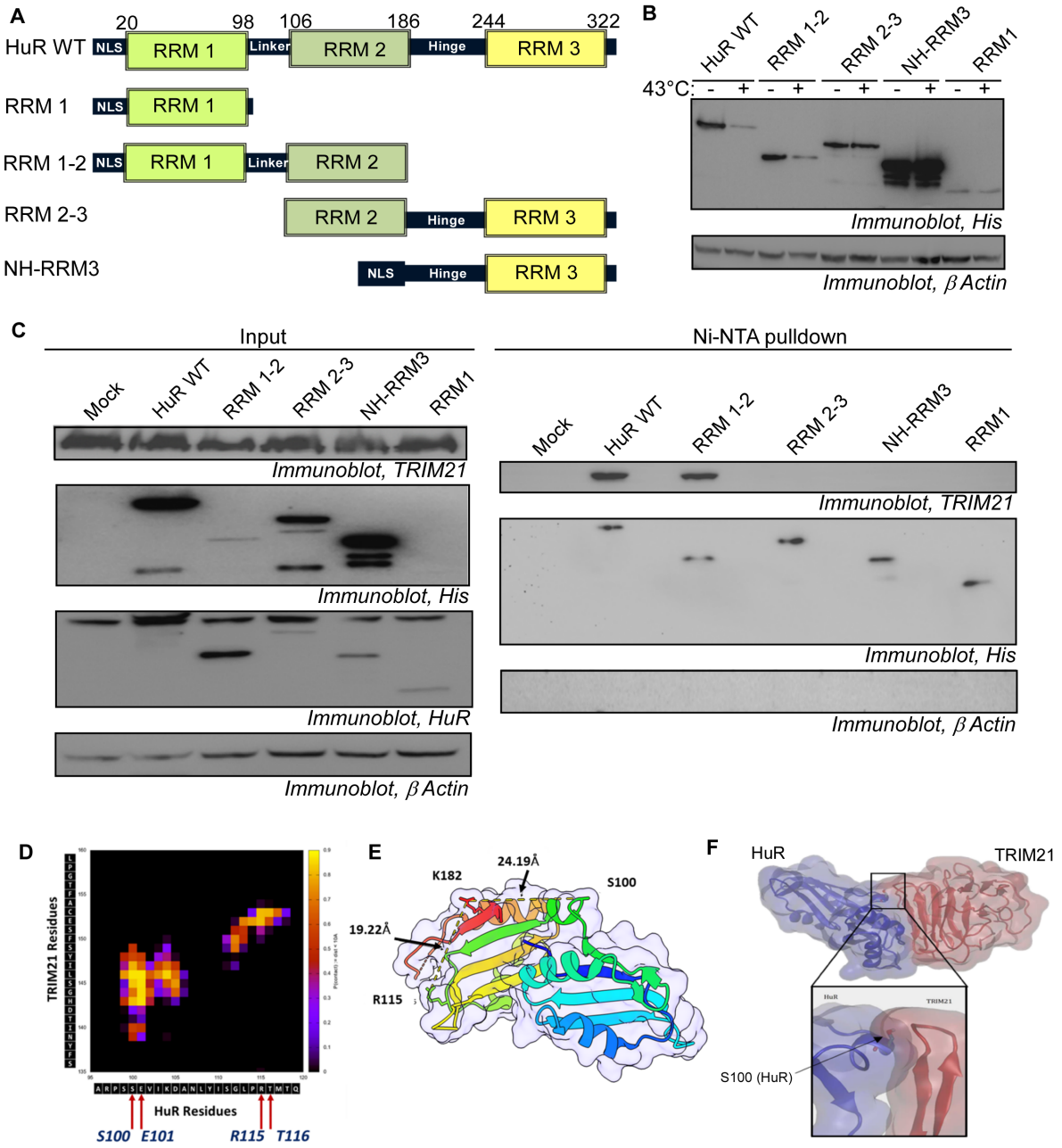

Figure 3

S100 and E101 residues of HuR are determinants of recognition by TRIM21. (**A**) Schematic representation of HuR WT and deletion constructs, indicating the 3 RNA recognition motifs (RRMs), nuclear localization signal (NLS), linker and hinge regions of HuR. (**B**) Immunoblot of lysates of MCF7 cells expressing His-tagged HuR WT and various His- tagged deletion mutants either exposed or unexposed to heat shock at 43°C for 2 h, probed with antibodies against the His tag and β Actin. (**C**)

MCF7 cells coexpressing TRIM21 with either His-tagged HuR WT or the various deletion mutants were exposed to heat shock at 43°C for 1 h in presence of MG132. Lysates were subjected to Ni-NTA affinity pulldown and the precipitates were immunoblotted with TRIM21, His and β Actin antibodies. Left panels represent the input lysates probed with the same antibodies along with HuR antibody. (**D**) Contact map of HuR residues with TRIM21 counterparts generated by MD simulation, contact being defined as a distance less than 10 Å between respective α-carbons of amino acids. (**E**) Structure of HuR RRM1-2 (PDB: 4EGL) showing the molecular distance between S100 and K182 and also between R115 and K182 residues. (**F**) A still from the MD simulation showing the bound state of RRM1-2 domain of HuR (blue) with the PRYSPRY domain of TRIM21 (red). The zoomed-in image shows the close contact between S100 of HuR (licorice structure) and the PRYSPRY domain of TRIM21.

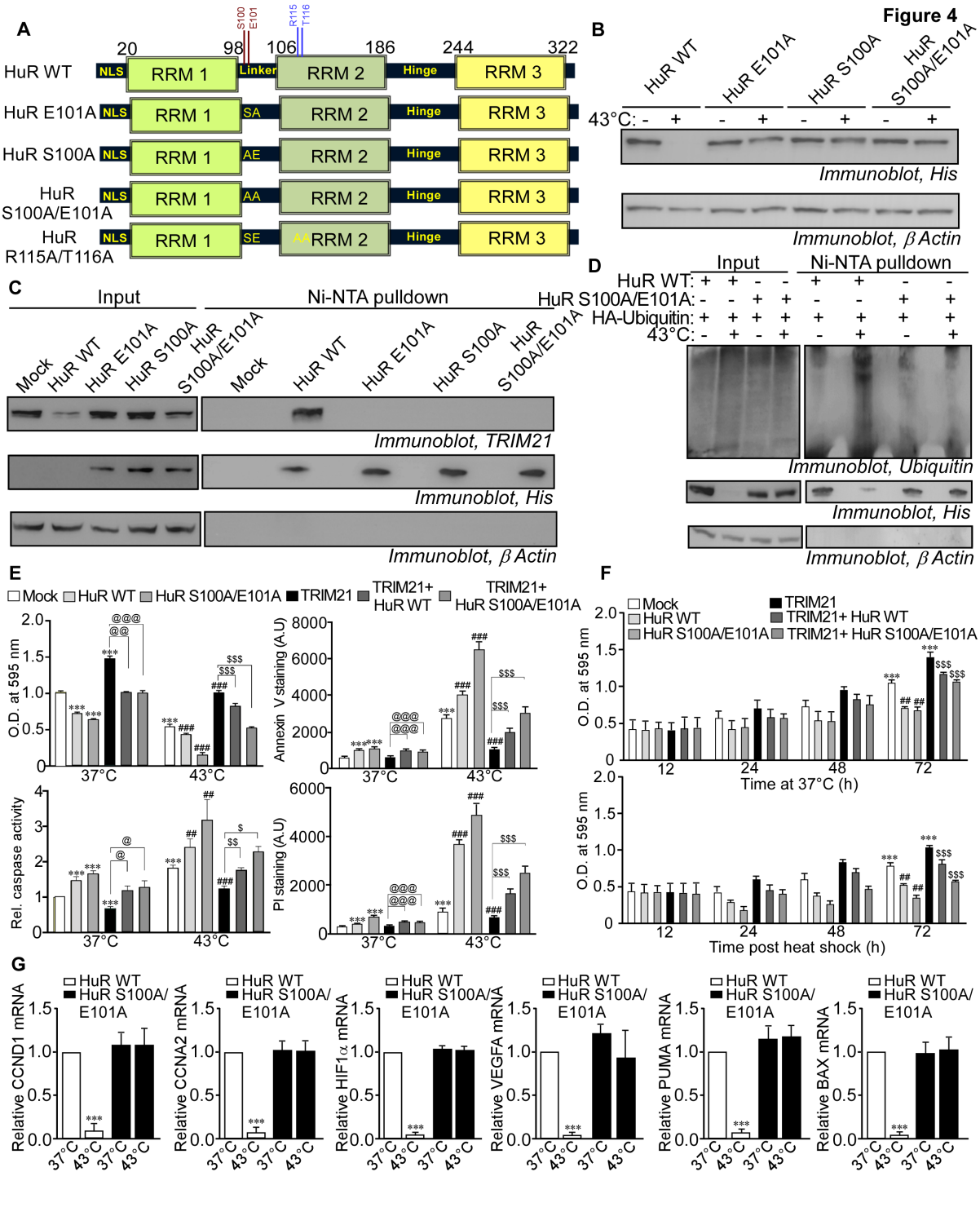

Figure 4

S100 and E101 residues of HuR determine TRIM21 binding and degradation of HuR under heat shock.

(**A**) Schematic representation of HuR WT and point mutants indicating the point mutations S100A, E101A, S100A/E101A double mutant and R115A/T116A double mutant. (**B**) Immunoblot of lysates of MCF7 cells expressing either His-tagged HuR WT or HuR E101A or HuR S100A or HuR S100A/E101A

mutant exposed or unexposed to heat shock at 43°C for 2 h, probed with antibodies against His tag and β Actin. (**C**) Lysates of MCF7 cells expressing TRIM21 together with either His-tagged HuR WT or HuR E101A or HuR S100A or HuR S101A/E101A mutant proteins exposed to heat shock at 43°C for 1 h in presence of MG132 were subjected to Ni-NTA affinity pulldown and the precipitates were immunoblotted with TRIM21, His and β Actin antibodies. Left panels represent the input lysates probed with the same antibodies. (**D**) Lysates of MCF7 cells expressing HA-tagged Ubiquitin together with either His tagged HuR WT or HuR S100A/E101A mutant proteins, exposed to heat shock at 43°C for 1 h in presence of MG132 were subjected to Ni-NTA affinity pulldown and the precipitates were immunoblotted with Ubiquitin, His, and β Actin antibodies. Left panels represent the input lysates probed with the same antibodies. (**E**) MCF7 cells transfected with either empty vector (Mock), HuR WT, HuR S100A/E101A and TRIM21 expression constructs individually or in combination were unexposed or exposed to heat shock at 43°C for 2 h. MTT assay was performed immediately post 2 h of heat shock (top left panel). Caspase 3/7 activity assay with a luminescent substrate was performed with MCF7 cells transfected with the same combinations of expression constructs and unexposed or exposed to heat shock at 43°C for 2 h. RLU values of each sample are expressed as fold change from that of mock-transfected cells at 37°C, taken as 1 (bottom left panel). Data represent mean ± SD values from three independent experiments for both panels. MCF7 cells transfected with the same combinations of plasmid DNA and exposed or not exposed to heat shock for 2 h, were stained with AnnexinV-AlexaFluor488 and PI to detect apoptosis by fluorescent microscopy. Fluorescence intensity of the Annexin V (top right panel) and PI stained (bottom right panel) cells was measured. Data represent mean ± SEM values from 100 cells randomly selected from each experimental setup. * represent significant difference from mock-transfected cells at 37°C, @ represent significant difference from TRIM21-expressing cells at 37°C, # represents significant difference from mock-transfected cells at 43°C and $ represents significant difference with respect to TRIM21-expressing cells at 43°C in all panels (paired two-tailed t-test). (**F**) MCF7 cells transfected with either empty vector (Mock), HuR WT, HuR S100A/E101A and TRIM21 expression constructs individually or in combination were unexposed (upper panel) or exposed (lower panel) to heat shock at 43°C for 2 h, following which they were allowed to grow at 37°C for 72 h. MTT assay was performed at the indicated time points. Data represent mean ± SD values from three independent experiments. *** represents significant difference (p-value ≤0.005) from mock-transfected cells and from TRIM21-expressing cells from the 12 h time point, ## represents significant difference (p-value ≤0.01) with respect to mock-transfected cells and $$$ represents significant difference (p-value ≤0.005) with respect to TRIM21 transfected cells from the 72 h time point (paired two-tailed t-test). (**G**) MCF7 cells were transfected with HuR WT or HuR S100A/E101A expressing constructs and exposed or not exposed to heat shock at 43°C for 2 h. mRNA expression levels of HuR targets, namely CCND1, CCNA2, HIF1A, VEGF, PUMA and BAX, were determined by quantitative RT-PCR using target specific primers from total RNA isolated from these cells. GAPDH mRNA was used as normalization control. The data represents fold change in target mRNA transcripts from that in mock transfected cells at 37°C, taken as 1. Data represents mean ± SD values from three independent experiments. *** signifies p value ≤ 0.005 (paired two-tailed t-test).

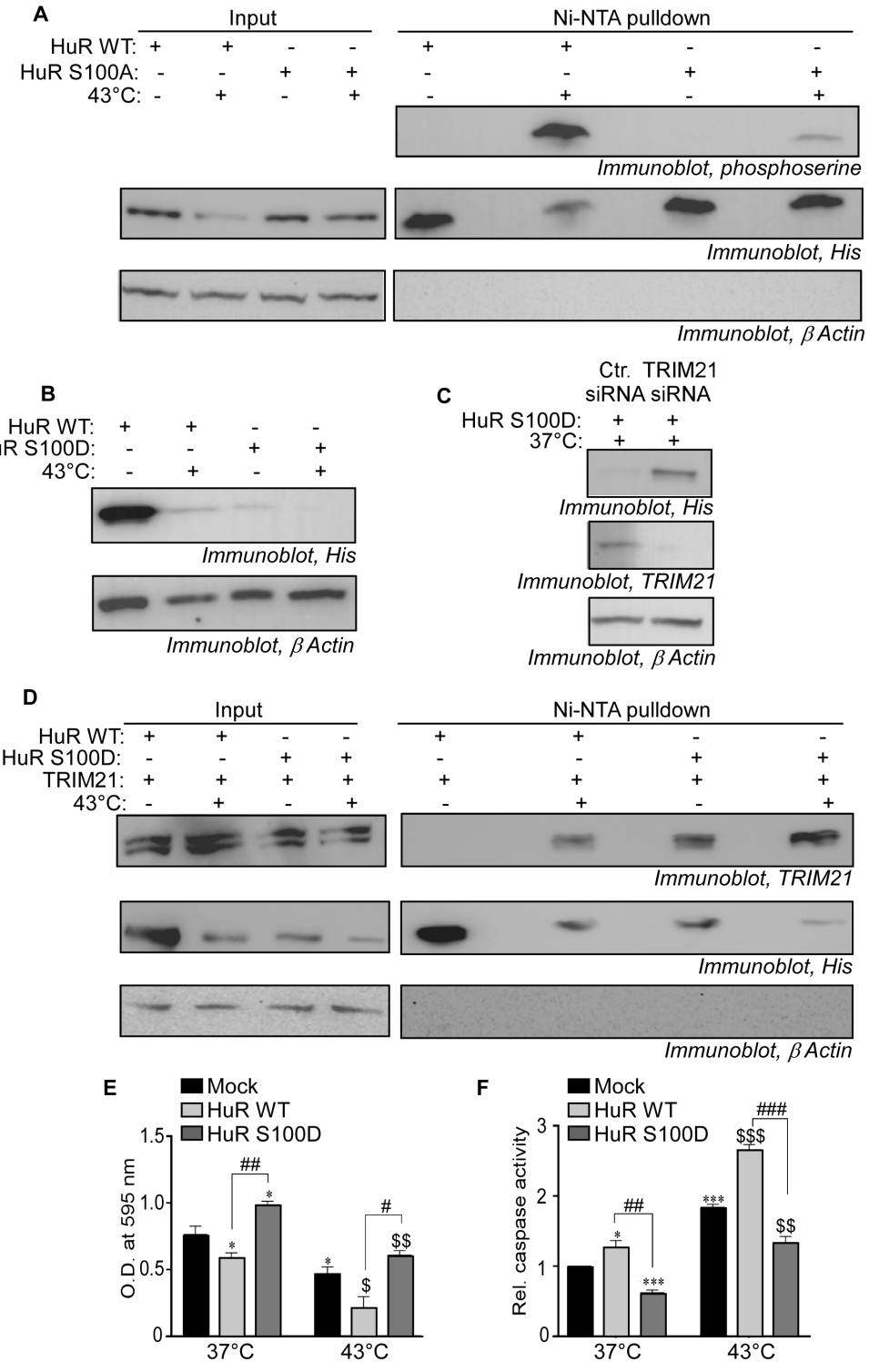

Figure 5

S100 phosphorylation is required for TRIM21 binding and degradation of HuR under heat shock. (**A**) Lysates of MCF7 cells expressing His-tagged HuR WT or HuR S100A mutant proteins exposed to heat shock at 43°C for 1 h in presence of MG132 were subjected to Ni-NTA affinity pulldown and the precipitates were immunoblotted with phosphoserine, His and β Actin antibodies. Left panels represent the input lysates probed with His and β Actin antibodies. (**B**) Immunoblot of lysates of MCF7 cells

expressing His-tagged HuR WT or HuR S100D mutant proteins exposed or not exposed to heat shock at 43°C for 2 h and probed with antibodies against His tag and β Actin. (**C**) Immunoblot of lysates of MCF7 cells transfected with control siRNA or siTRIM21 together with His-tagged HuR S100D expression construct and not exposed to heat shock, probed with antibodies against TRIM21, His tag and β Actin. (**D**) Lysates of MCF7 cells expressing TRIM21 and His-tagged HuR WT or HuR S100D mutant proteins exposed to heat shock at 43°C for 1 h in presence of MG132 were subjected to Ni-NTA affinity pulldown and the precipitates were immunoblotted with TRIM21, His and β Actin antibodies. Left panels represent the input lysates probed with the same antibodies. (**E**) MCF7 cells transfected with either empty vector (Mock), HuR WT or HuR S100D expression constructs were not exposed or exposed to heat shock at 43°C for 2 h. MTT assay was performed immediately post 2 h of heat shock. Data represent mean ± SD values from three independent experiments. * represents significant difference (p-value ≤0.05) from mock-transfected cells at 37°C, $ and $$ represent significant difference (p-value ≤0.05 and ≤0.01 respectively) from mock-transfected cells at 43°C, # and ## represent significant difference (p-value ≤ 0.05 and ≤0.01 respectively) between HuR WT-expressing cells and HuR S100D- expressing cells at 37°C and 43°C (paired two-tailed t-test). (**F**) MCF7 cells transfected with either empty vector (Mock), HuR WT or HuR S100D expression constructs were unexposed or exposed to heat shock at 43°C for 2 h. Caspase 3/7 activity assay with a luminescent substrate was performed. Relative light unit values of each sample, representing caspase 3/7 activity, are expressed as fold change from that of mock transfected cells at 37°C, taken as 1. Data represent mean ± SD values from three independent experiments. *, *** represent significant difference (p-value ≤ 0.05 and ≤0.005 respectively) from mock-transfected cells at 37°C,

and

$ represent significant difference (p-value ≤0.01 and ≤0.005 respectively) from mock-transfected cells at 43°C and ##, ### represent significant difference (p-value ≤0.01 and ≤0.005 respectively) between HuR WT expressing cells and HuR S100D expressing cells at 37°C and 43°C (paired two-tailed t-test).

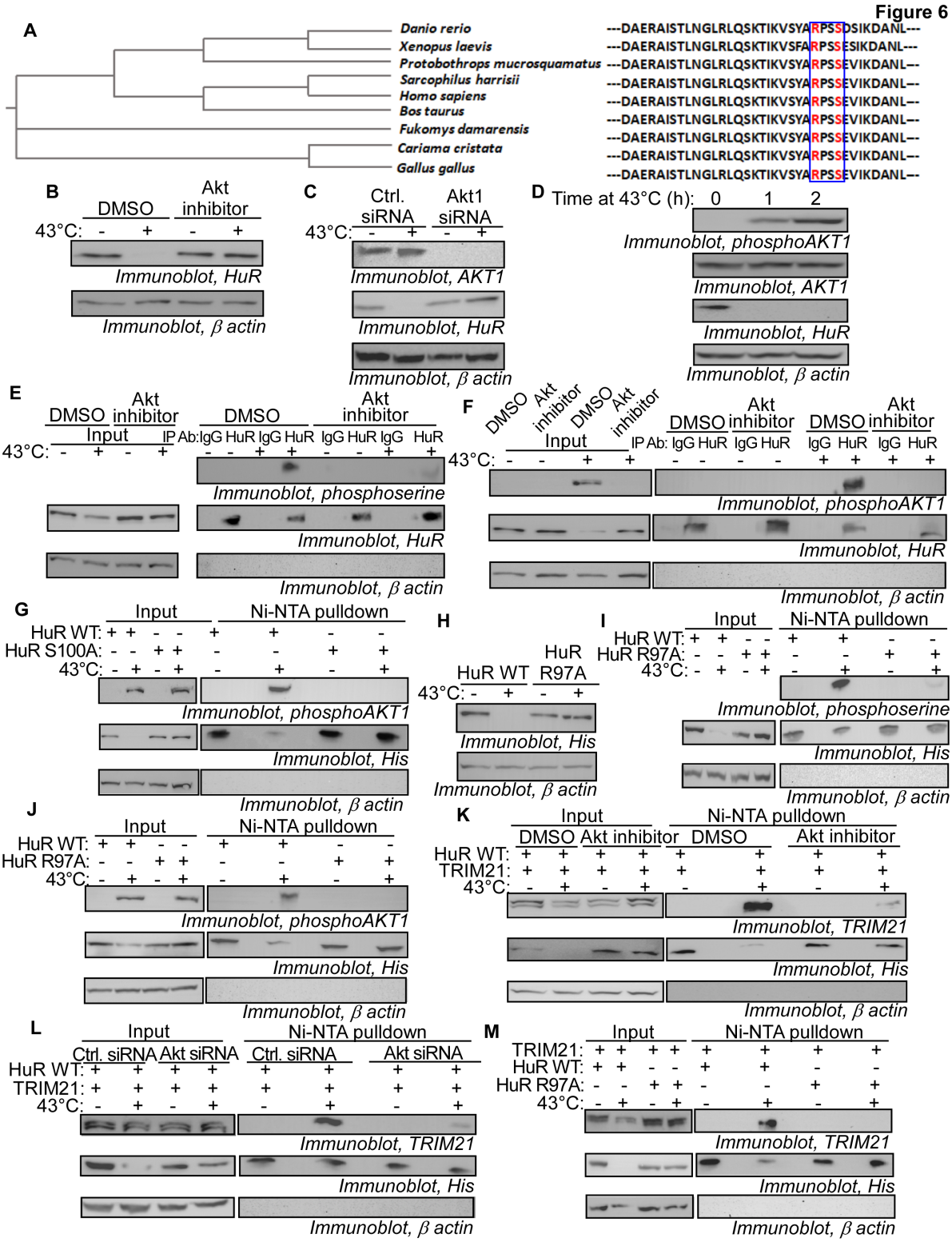

Figure 6

AKT1 phosphorylates S100 leading to TRIM21-mediated degradation of HuR under heat shock. (A) Phylogenetic analysis of HuR sequences from vertebrate species showing evolutionary conservation of AKT1 target consensus motif (RXXS/T). (B) Immunoblot of lysates of MCF7 cells treated with DMSO or 10 μM Akt1 inhibitor for 2 h and subsequently not exposed or exposed to heat shock at 43°C for 2 h, probed with antibodies against HuR and β Actin. (C) Immunoblot of lysates of MCF7 cells transfected

with control siRNA or Akt1 siRNA, and unexposed or exposed to heat shock at 43°C for 2 h, post 48 h of siRNA transfection, probed with antibodies against AKT1, HuR and β Actin. (D) Immunoblot of lysates of MCF7 cells exposed to heat shock at 43°C for the indicated time durations, probed with antibodies against phosphoAKT1, AKT1, HuR and β Actin. (E) MCF7 cells were treated with DMSO or 10 μM Akt Inhibitor for 2 h followed by 1 h MG132 treatment, and unexposed or exposed to heat shock at 43°C for 2 h. Cell lysates were immunoprecipitated with non-immune IgG and HuR antibody and the immunoprecipitates were probed with phosphoserine, HuR and β Actin antibodies. Left panels represent the input lysates probed with HuR and β Actin antibodies. (F) Lysates of MCF7 cells treated with DMSO or 10 μM Akt inhibitor for 2 h and MG132 for 1 and not exposed or exposed to heat shock at 43°C for 2 h, were immunoprecipitated with non-immune IgG and HuR antibody and the immunoprecipitates were probed with phosphoAKT1, HuR and β Actin antibodies. Left panels represent the input lysates probed with the same antibodies. (G) Lysates of MCF7 cells expressing His-tagged HuR WT or HuR S100A and treated with MG132 and unexposed or exposed to heat shock at 43°C for 1 h, were subjected to Ni-NTA affinity pulldown. The precipitates were probed with antibodies against phosphoAKT1, His and β Actin. Left panels represent the input lysates probed with the same antibodies. (H) Immunoblot of lysates from MCF7 cells expressing His-tagged HuR WT or HuR R97A mutant proteins, not exposed or exposed to shock at 43°C for 2 h, probed with antibodies against His tag and β Actin. (I) Lysates of MCF7 cells expressing His-tagged HuR WT or HuR R97A and treated with MG132 and unexposed or exposed to heat shock at 43°C for 1 h, were subjected to Ni-NTA affinity pulldown. The precipitates were probed with antibodies against phosphoserine, His and β Actin. Left panels represent the input lysates probed with the same antibodies. (J) Lysates of MCF7 cells expressing His-tagged HuR WT or HuR R97A and treated with MG132 and not exposed or exposed to heat shock at 43°C for 1 h, were subjected to Ni-NTA affinity pulldown. The precipitates were probed with antibodies against phosphoAKT1, His and β Actin. Left panels represent the input lysates probed with the same antibodies. (K) MCF7 cells were co-transfected with TRIM21 and His-tagged HuR WT expression constructs, treated with 10 μM Akt Inhibitor for 2 h followed by 1 h MG132 treatment, and unexposed or exposed to heat shock at 43°C for 2 h. Cell lysates were subjected to Ni-NTA affinity pulldown and the precipitates were immunoblotted with TRIM21, His and β Actin antibodies. Left panels represent the input lysates probed with the same antibodies. (L) MCF7 cells were co-transfected with TRIM21 and His-tagged HuR WT expression constructs along control siRNA or Akt1 siRNA. Post 46 h of transfection and 1 h of MG132 treatment, cells were not exposed or exposed to heat shock at 43°C for 1 h. Lysates were subjected to Ni-NTA affinity pulldown and the precipitates were immunoblotted with TRIM21, His and β Actin antibodies. Left panels represent the input lysates probed with the same antibodies. (M) Lysates of MCF7 cells expressing TRIM21 together with His-tagged HuR WT or HuR R97A and treated with MG132 and unexposed or exposed to heat shock at 43°C for 1 h, were subjected to Ni-NTA affinity pulldown. The precipitates were probed with antibodies against TRIM21, His and β Actin. Left panels represent the input lysates probed with the same antibodies.

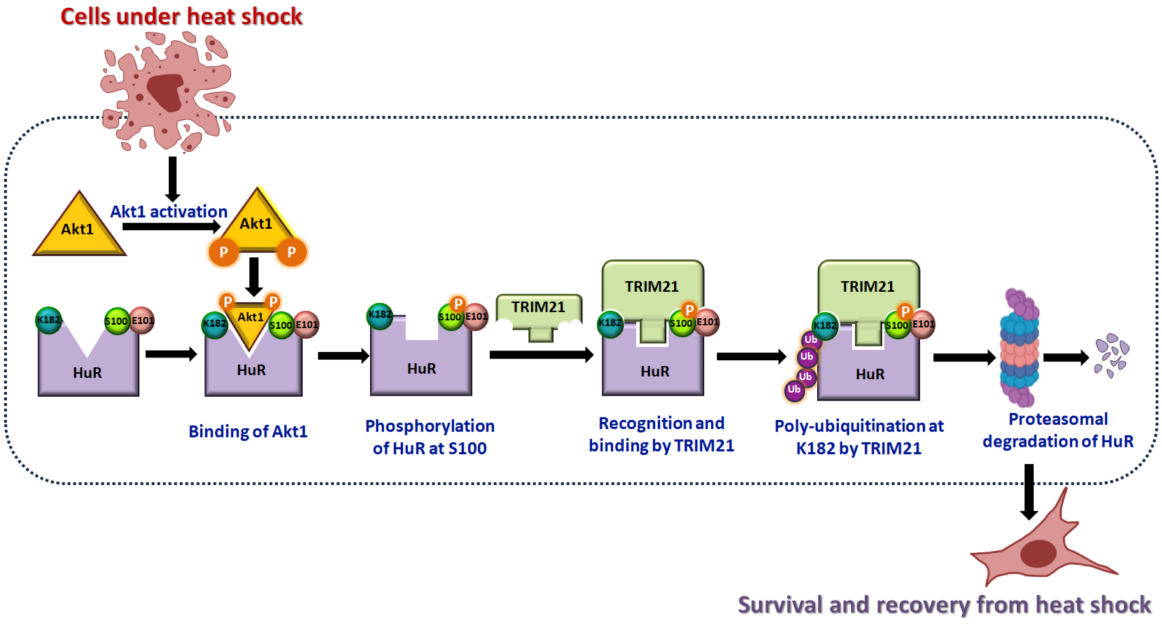

Figure 7

Concerted action by AKT1 and TRIM21 causes HuR degradation under heat shock. Proposed model showing the sequential actions of AKT1 and TRIM21 under heat shock, leading to phosphorylation of HuR on S100 and ubiquitination on K182, generating a heat-shock induced “phosphodegron” in HuR. This leads to the proteasomal degradation of HuR allowing cell survival and adaptation to heat shock.

Supplementary Files

This is a list of supplementary files associated with this preprint. Click to download.

- SupplFiguresCDD.pdf